10. A. Hjortsberg, I. Hamberg, and C. G. Granqvist, *Thin Solid Films* **90**, 323 (1982).

11. M. Mizuhashi, *Thin Solid Films* **70**, 91 (1980).

12. A. Dietrich, K. Schmalzbauer, and H. Hoffmann, *Thin Solid Films* **122**, 19 (1984).

13. J. A. Dobrowolski *et al.*, *Appl. Opt.* **26**, 5204 (1987).

2.B Transient-Surface Debye-Waller Effect

In the study of the interactions of ultrafast lasers with surfaces and the subsequent reactions, a key parameter is the time evolution of the surface temperature. Typically, this is determined for simple systems using a solution of the heat-diffusion equation. However, even in the simplest cases (e.g., the heating of a crystal surface that undergoes no phase change), such a solution may only provide the time evolution of the surface temperature with poor accuracy since many assumptions are built into these models. These assumptions include the temperature behaviors of the specific heat of the laser-irradiated material, its thermal conductivity, and laser-energy coupling. It has been previously demonstrated that second-harmonic generation at surfaces could be used as a surface structural probe[1] and, when resonantly enhanced, can also be used as a surface-temperature probe.[2] Surface temperatures deduced from the resonantly enhanced second-harmonic generation from an Ag(110) surface heated with nanosecond laser pulses have shown agreement with a heat-diffusion model.[2] However, this approach does not offer a general technique suitable to time-resolve the evolution of the surface temperature for different materials. Here we demonstrate the utilization of picosecond time-resolved reflection high-energy electron diffraction (RHEED) as a surface-lattice temperature probe.

Electron diffraction (both high energy and low energy) is a well-developed surface structural probe and has been utilized for many decades in surface studies.[3–7] The development of a picosecond-transmission electron-diffraction system was reported several years ago.[8] More recently we have demonstrated picosecond RHEED.[9] A detailed description of our ultrahigh vacuum picosecond RHEED system is given in Ref. 10.

Picosecond RHEED—A Surface-Temperature Probe

The basic idea of this technique is the utilization of a picosecond laser pulse to create an electron pulse with a comparable time duration. A schematic diagram of this technique is shown in Fig. 43.31. We use a Nd:YAG laser (λ = 1.06 μm) to irradiate the sample, while the electron probing pulse is generated by irradiation of a photocathode with the frequency-quadrupled Nd:YAG (λ = 0.266 μm). The photogenerated electrons are collimated and focused electrostatically making them suitable to obtain a good RHEED pattern from the studied crystal surface. Only a very small part of the Nd:YAG fundamental is converted to the ultraviolet; thus, most of the laser energy is available to irradiate the sample. By spatially delaying the fundamental from the ultraviolet laser pulse, it is possible to obtain RHEED patterns at times before, during, and after laser irradiation with up to a few-hundred-picoseconds time resolution.

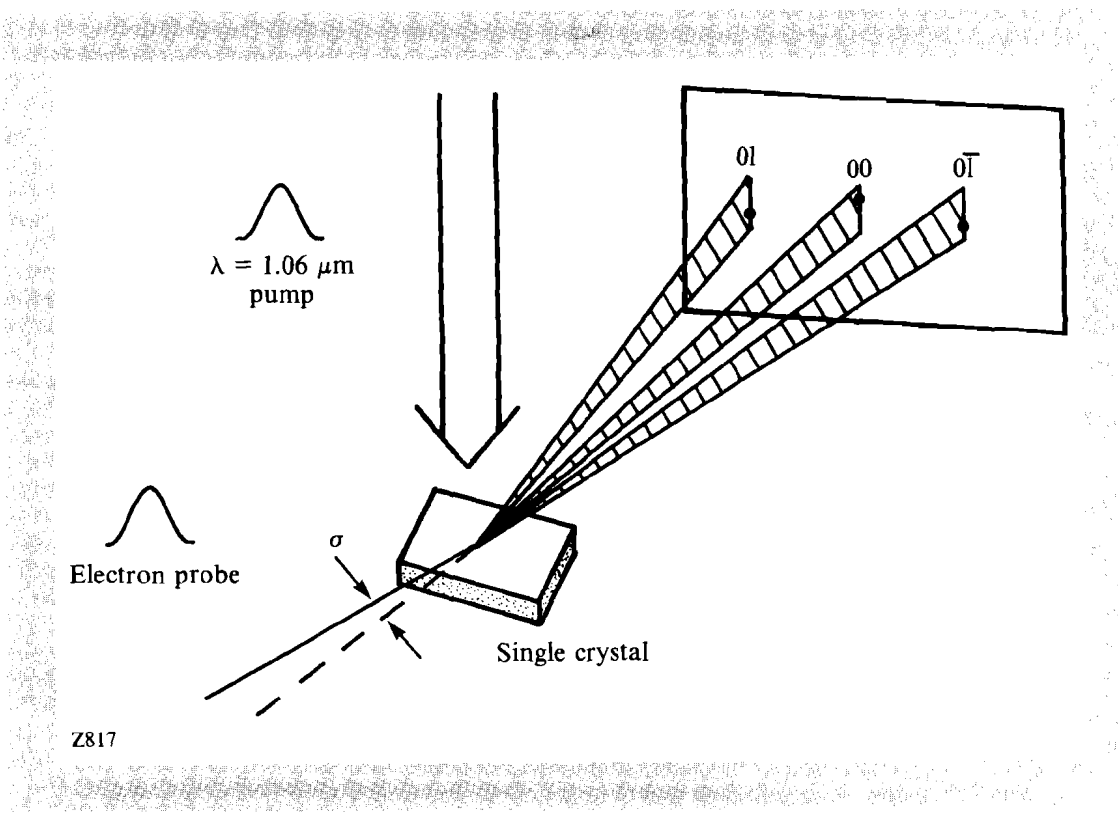

Fig. 43.31
Picosecond time-resolved reflection high-energy electron diffraction (RHEED). The laser pump and electron probe are well synchronized.

The sensitivity of the diffraction pattern to temperature comes from the fact that as the temperature is raised, there is an increased atomic vibrational amplitude and, thus, an increased dephasing of the atomic scattering centers. This dephasing on the diffraction pattern reduces the number of electrons elastically scattered (i.e., to reduce the diffraction streak intensity). The reduced streak intensity shows up as an increased background that is

caused by the inelastically scattered electrons. Such a reduced intensity occurs with no widening of the diffraction streaks (or spots). This is known as the Debye-Waller effect, which was first analyzed by Debye for x-ray diffraction.[11]

Experimental Setup

The design of the photoactivated RHEED electron gun is similar to that of an x-ray streak camera. A 250-Å gold film deposited on a sapphire window is used as a photocathode. A single electrostatic lens is used to collimate and focus the electrons. A schematic diagram of the electron gun is shown in Fig. 43.32. For the current experiment, 14-keV electrons are used. The electrons are focused to a spot size of ~340 μm and have a pulse width comparable to the pulse width of the laser. Approximately 10^5 electrons are contained in each pulse.

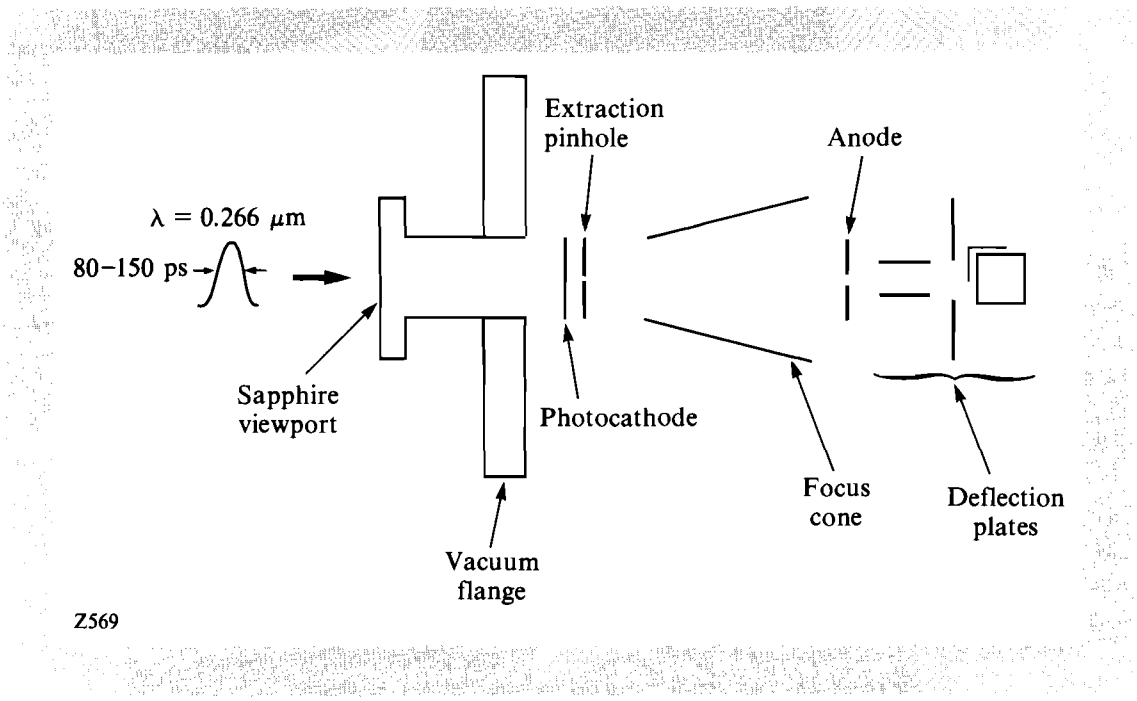

Fig. 43.32
A schematic of the photoactivated picosecond electron gun.

The picosecond RHEED system is assembled on a dedicated ultrahigh vacuum system (10^{-10} Torr). Conventional techniques of sample cleaning by argon-ion bombardment and annealing are performed prior to experiments.

A schematic diagram of the laser system used to drive the picosecond RHEED apparatus is shown in Fig. 43.33. A cw-pumped, mode-locked, Nd:YAG (λ = 1.06 μm) oscillator generates a 100-MHz train of about 120- to 300-ps FWHM pulses. A switchout consisting of a Pockels cell and two polarizers is used to select a pulse at a variable repetition rate up to

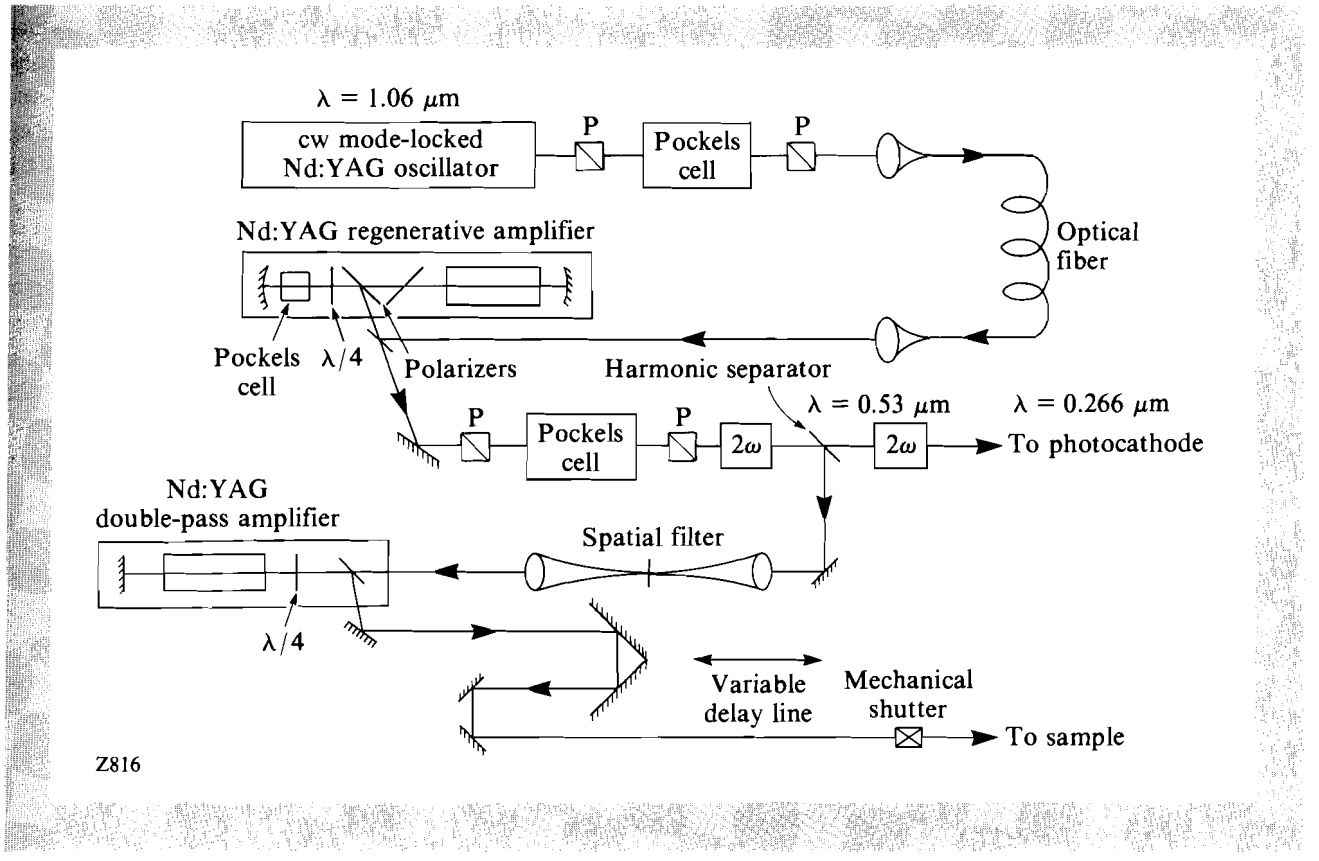

Fig. 43.33
A schematic diagram of the laser system driving the picosecond RHEED apparatus.

1.5 kHz. The selected oscillator pulse is coupled to the cw-pumped regenerative amplifier.[12] Pulse injection is accomplished by applying a fast step to the Pockels cell in the regenerative amplifier cavity.[13] The magnitude of this voltage step is to achieve quarter-wave retardation. This causes a cavity round trip of full-wave retardation, thus minimizing cavity losses and trapping the injected pulse. After ~40 round trips, the pulse inside the regenerative-amplifier cavity builds up to its peak value and is cavity dumped by applying a second voltage-step function causing the Pockels cell to have half-wave retardation.[13]

The laser pulse width from the regenerative amplifier is nearly equal to that of the oscillator; that is, pulse broadening in the regenerative amplifier is negligible. The pulse width can vary from day to day, depending on the alignment of the mode-locker and setting of the cavity length.

The energy content of the principal pulse is typically ~0.4 mJ. To increase the ratio of the energy content of the principal pulse to that of other pulses, an external switchout consisting of a Pockels cell and two polarizers is used. After the external switchout, the ratio is observed to be better than several hundred to one.

The output of the external Pockels cell is frequency doubled. Less than 1% conversion efficiency is needed. The fundamental and the frequency-doubled Nd:YAG pulses are split in a harmonic separator. The green ($\lambda = 0.53\ \mu$m) pulses are further doubled to generate ultraviolet pulses ($\lambda = 0.266\ \mu$m). These ultraviolet photons are utilized to pump the photocathode.

The fundamental pulse is spatially filtered and passes through a 7-mm double-pass amplifier. During system alignment, the double-pass amplifier is not activated; for heating experiments, the double-pass amplifier is activated. This is typically operated up to 30 mJ at an 8-Hz repetition rate. An optical delay line is used to vary the timing between the fundamental pulse and the ultraviolet pulse that drives the photocathode of the electron gun.

For electron detection, we use gated microchannel plates (MCP's) proximity focused to a P-47 phosphor screen. Since laser heating below the threshold of surface damage is reversible, we can average over many shots to enhance our signal. The maximum repetition rate of this system when no MCP's are used is limited only by the laser repetition rate, since the decay time of the P-47 phosphor screen is ~0.15 μs. When MCP's are used, the maximum repetition rate is limited by their dead time that typically limits the system to a few kilohertz.[14]

To obtain quantitative information on surface structure and temperature from the picosecond RHEED patterns, it is necessary to determine the scattering angles and the diffraction intensity. For the current experiments we use a linear array detector, an optical multichannel analyzer (OMA), to observe a line across the diffraction pattern. A RHEED pattern of the Pb(110) surface obtained by using picosecond electron pulses is shown in Fig. 43.34. The approximate location of the line scan across the image observed by the OMA is indicated.

Measurements of Transient Debye-Waller Effect

We have performed measurements of the surface Debye-Waller effect with a few-hundred-picosecond time resolution on a Pb(110) crystal. By measuring the distance from the undiffracted electron beam to the pattern's shadow edge and knowing the distance of the phosphor screen assembly to the sample, we estimate the electron beam's angle of incidence on the sample to be ~3°. The $\lambda = 1.06\ \mu$m fundamental is used to heat the surface of the crystal (at near normal incidence), while the electron pulses are used to probe the surface in the manner previously described. The system is operated at 8-Hz repetition rate and provides a maximum energy of ~20 mJ per pulse to the surface of the sample. The infrared heating pulse passes through an optical delay line before hitting the sample. The timing of the heating laser pulse and the electron pulse at the sample is set by adjustments of the delay line.

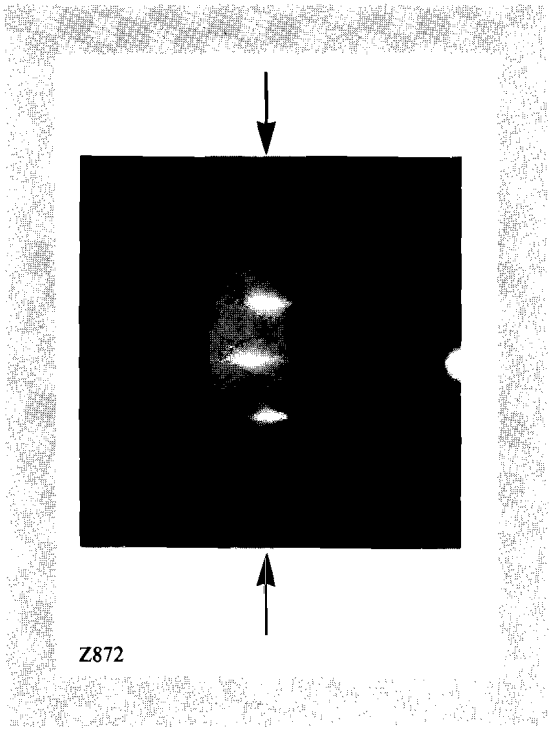

Fig. 43.34
A RHEED pattern of Pb(110) taken using many picosecond electron pulses. The arrows indicate the approximate location of the line scan obtained by lens imaging this pattern onto an optical multichannel analyzer (OMA).

To enhance our signal, we insert a mechanical shutter in the IR beam path that allows every other laser-heating pulse to interact with the sample. Two line scans are obtained for determined experimental conditions: the first is with no laser heating; the second is with laser heating. Each scan is stored in a separate memory. This process is repeated at various positions of the delay line. Scans with and without laser heating are sorted and averaged in separate memories. This averaging effectively compensates for shot-to-shot fluctuations and for long-term drifts in the UV laser intensity and electron gun. However, pulse-to-pulse fluctuations and long-term drifts in the heating IR pulse cannot be compensated for using this method. A histogram of the laser-heating pulse energy indicates that, for about 90% of the pulses, the pulse energy falls within ±10% of the average. Long-term stability of the heating laser is regularly monitored during the experiment.

For a representative experiment, line scans through the diffraction pattern obtained at various times relative to the arrival of the laser-heating pulse to the sample are shown in Fig. 43.35. The relative peak heights are determined by the crystal alignment and the positioning of the linear array detector. The upper scans correspond to no laser heating while the lower scans correspond to the laser-heated surface. The OMA is set to average 480 shots per scan. From this figure, we can see that there is a significant change in the intensity of the diffraction rods as the laser-heating pulse strikes the sample. This change decreases as the surface of the sample cools mainly by heat diffusion to the bulk.

The time-resolved results are related to the lattice temperature by performing a static heating experiment. We heat the sample on a resistively

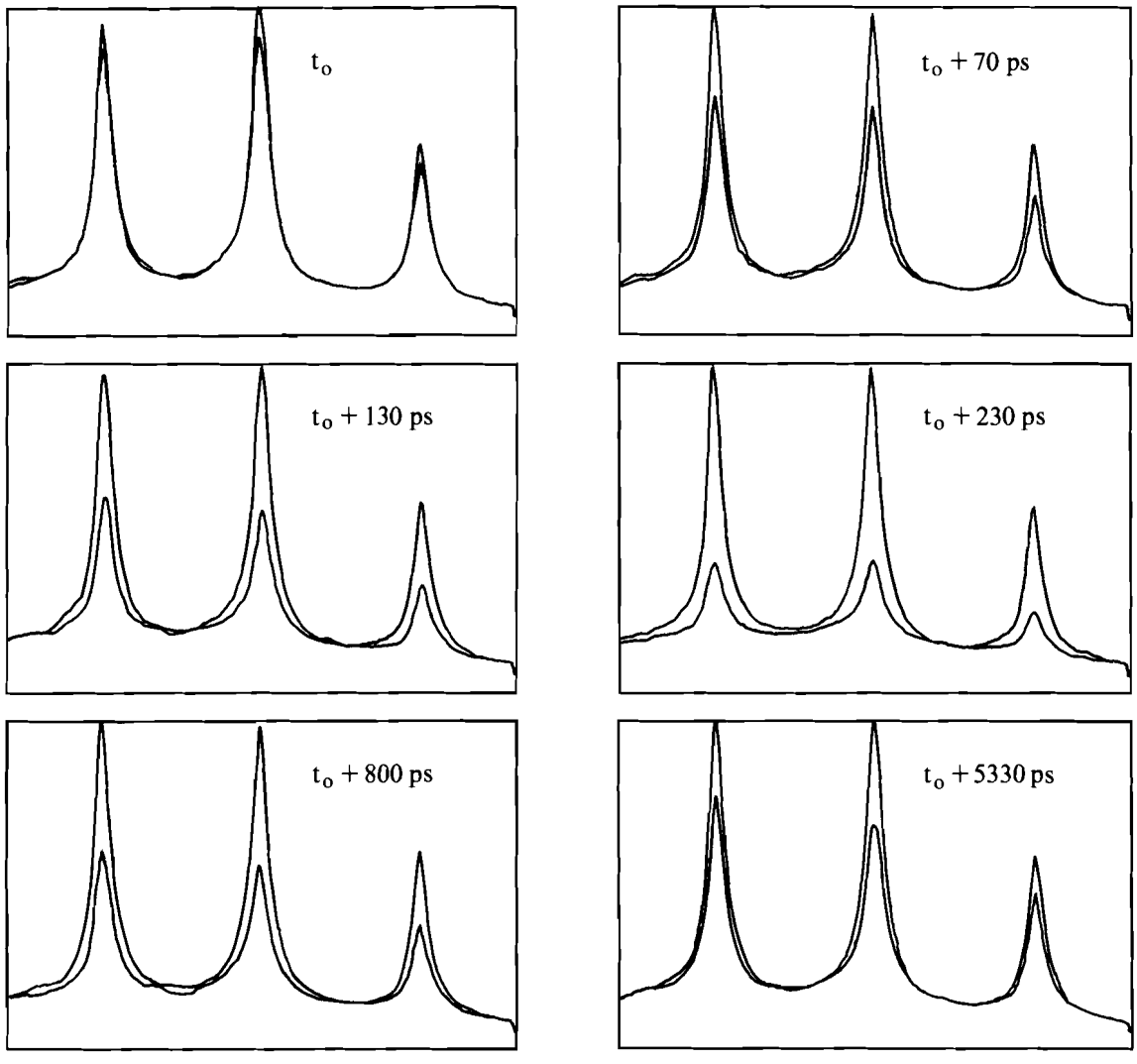

Fig. 43.35
Line scans through the diffraction patterns at various times. The upper scans correspond to an unheated surface while the lower scans correspond to a laser-heated surface.

heated stage and observe the intensity of the diffraction pattern as a function of the sample temperature, measured by thermocouples located on the surface of the stage just above and below the sample. In this way, we determine the normalized RHEED streak intensity when the sample is heated from room temperature to a given temperature. Results of such a measurement of the average change in one of the streaks (left peak in Fig. 43.35) are shown in Fig. 43.36, along with an exponential fit of the temperature versus RHEED streak intensity normalized to the room-temperature streak intensity. By comparing these intensity measurements

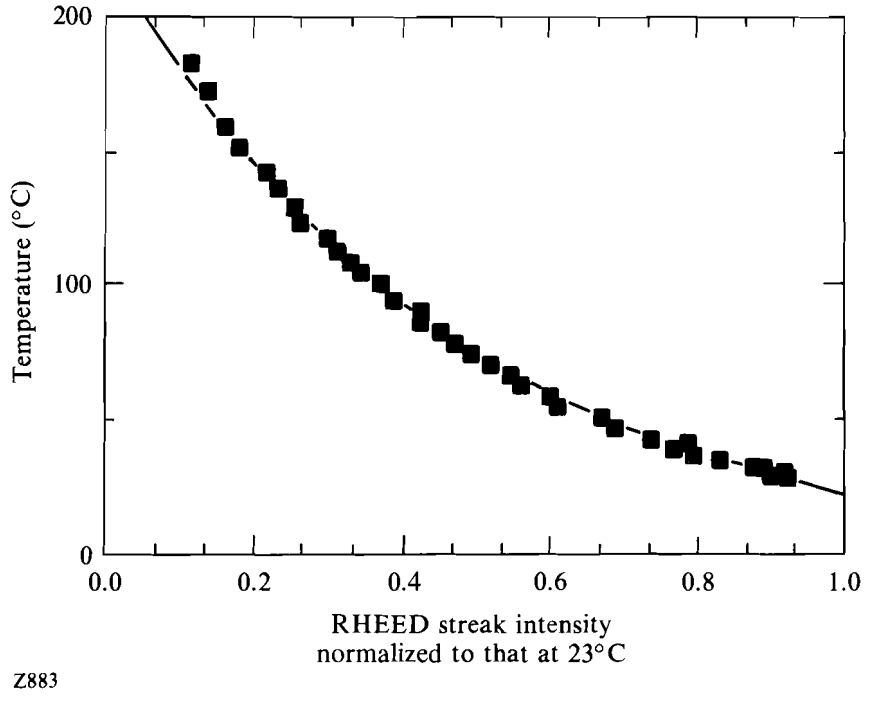

Fig. 43.36
Temperature versus normalized RHEED streak intensity. The Pb(110) sample is heated on a hot stage. The temperature is measured using thermocouples. The location of the line scan across the diffraction pattern is the same as that for pulsed laser heating. An exponential fit is made to the data and is used to obtain the time-resolved surface temperature in Fig. 43.37.

under different temperatures with measurements taken for picosecond laser heating, we obtain the time-resolved surface temperature with up to a few-hundred-picosecond time resolution. The validity of the temperature calibration, which is based on a comparison of the magnitude of the surface Debye-Waller effect measured under static conditions with that measured under dynamic heating conditions, was not directly tested. However, this calibration should hold if (1) the time scale of our measurements is longer than that needed for equilibrium to be established between the electrons and the lattice in our sample (in metals, at room temperature or higher, this typically occurs within a few picoseconds[15]); (2) no surface phase transformation occurs; and (3) no accumulated surface modifications occur by repeated laser heating. These conditions appear to be fulfilled in the experiments reported here.

Based on this calibration, we obtain the time evolution of the surface-temperature rise caused by laser heating. Results from an experimental run are shown in Fig. 43.37, along with the decay of the surface-temperature rise obtained from a heat-diffusion model.

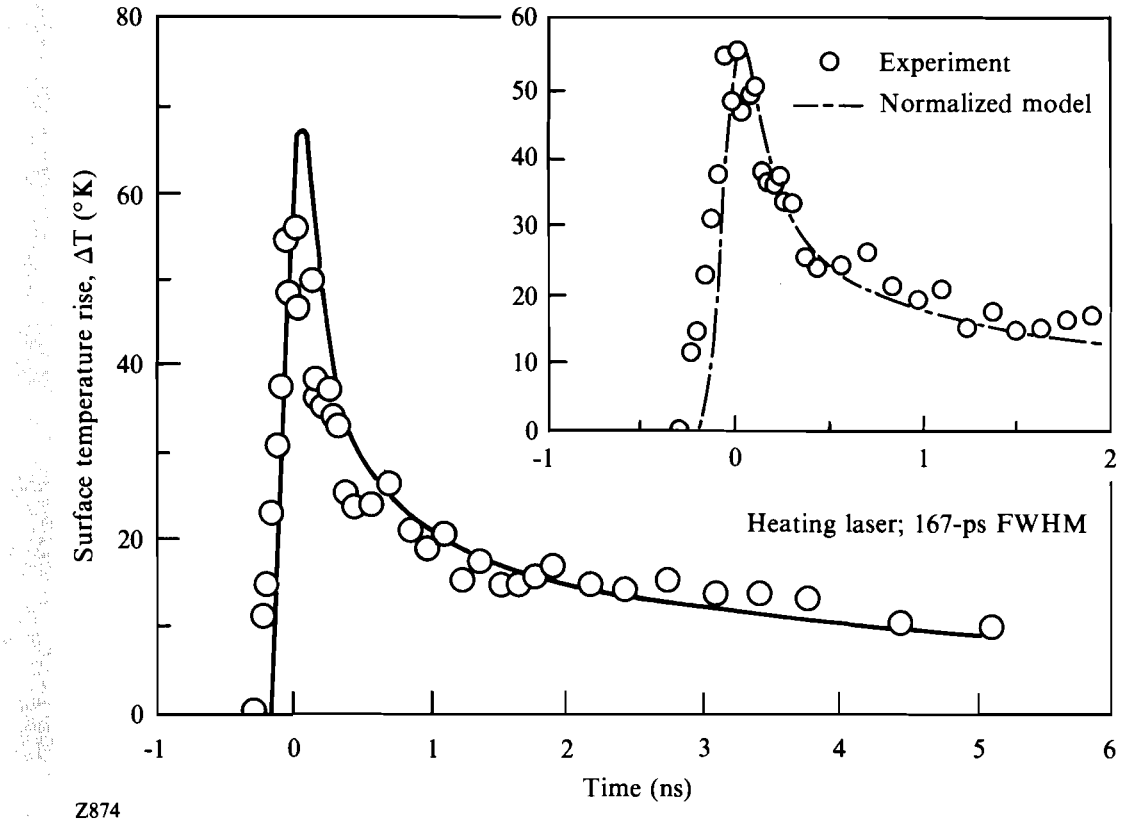

Fig. 43.37
Transient surface temperature rise of Pb(110) irradiated with 3.5×10^7 W/cm^2 peak intensity, 167-ps FWHM, Nd:YAG ($\lambda = 1.06\,\mu$m) laser pulses. Experimental results are obtained from the transient surface Debye-Waller effect on RHEED intensity using the calibration obtained in Fig. 43.36. The solid line is obtained from a numerical heat diffusion model. In the inset, the peak temperature from the model is normalized to that from the experiment.

Heat-Diffusion Model

A numerical solution of the surface temperature is obtained from a one-dimensional heat-diffusion model based on the equation[16]

$$C\left[dT(z,t)/dt\right] = K\left[d^2T(z,t)/dz^2\right] + I(1-R)\alpha e^{-\alpha z} f(t),$$

where C is the heat capacity per unit volume, $T(z,t)$ is the temperature profile at distance z normal to the sample surface ($z = 0$), t is time, K is the thermal conductivity, I is the laser peak intensity, α is the absorption per unit length, and $f(t)$ is the time dependence of the laser pulse that is assumed Gaussian. The values of parameters in this equation are listed in Table 43.II.

Table 43.II: Values of physical constants used for the calculation shown in Fig. 43.37.

C: Heat capacity per unit volume (J/m^3 K)[a]	1.47×10^6
K: Thermal conductivity (W/m K)[a]	34.6
I: Laser peak intensity (W/cm^2)	3.5×10^7
R: Reflectivity [b]	0.857
α: Absorption coefficient(m^{-1})[b]	6.77×10^7

(a) *Amercian Institute of Physics Handbook*, 3rd ed. (McGraw-Hill, New York, 1972).
(b) From $R = [(n-1)^2 + k^2]/[(n+1)^2 + k^2]$ and $\alpha = 4\pi k/\lambda$, where n and k are the real and imaginary parts of the complex index of refraction. [A. I. Golovashkin and G. P. Motulevich, *Sov. Phys. JETP* **26,** 881 (1968)].

Z895

As shown in Fig. 43.37, the surface-temperature rise obtained using the transient-surface Debye-Waller effect on the picosecond RHEED pattern shows general agreement with that predicted by a heat-diffusion model. However, an uncertainty in the model is the value of the reflectivity and absorptivity. For these values we have relied on the measurements of Golovashkin and Motulevich rather than measuring it for our sample. Nonlocal effects on the thermal conductivity, which can arise if the temperature gradient is significant within a mean-free path of the heat carriers,[17] i.e., hot electrons, are also not included in the model. Such nonlocal effects were shown to reduce heat conductivity.[17]

Conclusion

We have demonstrated the use of picosecond RHEED as a time-resolved surface-temperature probe. The temperature measurement is based on the surface Debye-Waller effect that results in a reduction of the number of elastically scattered electrons with lattice heating, thus reducing the RHEED streak intensity. Our time-resolved measurements of the picosecond-laser-heated Pb(1 1 0) surface show general agreement with a heat-diffusion model.

The time resolution, in the current experiments, is limited to a few hundred picoseconds. However, the extension of time-resolved RHEED techniques, as a temperature probe of recurrent events (e.g., simple surface heating), to a subpicosecond resolution should be possible. The technology required to accomplish this is similar to that currently utilized in subpicosecond streak cameras.[18] The temperature-measurement accuracy depends on the overall stability of the system and its repetition rate. For the data shown in Fig. 43.37 we estimate an accuracy of ±15 K. However, much higher accuracy can be

achieved by increasing the repetition rate and collecting data for a specific narrow window of laser-pulse energy.

The technique of picosecond RHEED offers both surface selectivity and temperature sensitivity. In addition to its utilization as a time-resolved structural and temperature probe of fast-surface processes, it can also be used to study the thermal properties of extremely thin films (up to a few monolayers).

ACKNOWLEDGMENT

This work was supported by the U. S. Department of Energy under contract No. DE-FG02-88ER45376 and by the United States Air Force Office of Scientific Research under contract No. AFOSR-87-0327. Additional support was provided by the Laser Fusion Feasibility Project at the Laboratory for Laser Energetics, which has the following sponsors: Empire State Electric Energy Research Corporation, New York State Energy Research and Development Authority, Ontario Hydro, and the University of Rochester.

REFERENCES

1. C. V. Shank, R. Yen, and C. Hirlimann, *Phys. Rev. Lett.* **51**, 900 (1983).
2. J. M. Hicks, L. E. Urbach, E. W. Plummer, and H.-L. Dai, *Phys. Rev. Lett.* **61**, 2588 (1988).
3. E. Bauer, *Techniques of Metal Research*, Vol. II, Part 2, edited by R. F. Bunshah (Interscience, New York, 1969), p. 501.
4. P. J. Estrup and E. G. McRae, *Surf. Sci.* **25**, 1 (1971).
5. C. B. Duke and R. L. Park, *Phys. Today* **25**, 23 (1972).
6. D. Lichtman, *Methods of Surface Analysis*, Vol. I, edited by A. W. Czanderna (Elsevier Sci. Pub., New York, 1975), p. 39.
7. A. U. MacRae, *Science* **139**, 379 (1963).
8. G. Mourou and S. Williamson, *Appl. Phys. Lett.* **41**, 44 (1982).
9. H. E. Elsayed-Ali and G. A. Mourou, *Appl. Phys. Lett.* **52**, 103 (1988).
10. H. E. Elsayed-Ali and J. W. Herman, *Rev. Sci. Instrum.* **61**, 1636 (1990).
11. C. Kittel, *Introduction to Solid State Physics*, 5th edition (Wiley, New York, 1976), p. 63.
12. I. N. Duling III, T. Norris, T. Sizer II, P. Bado, and G. A. Mourou, *J. Opt. Soc. Am. B* **2**, 616 (1985).
13. P. Bado and M. Bouvier, *Rev. Sci. Instrum.* **56**, 1744 (1985).
14. J. L. Wiza, *Nucl. Instrum. Methods* **162**, 587 (1979).

15. H. E. Elsayed-Ali, T. B. Norris, M. A. Pessot, and G. A. Mourou, *Phys. Rev. Lett.* **58**, 1212 (1987).

16. J. H. Bechtel, *J. Appl. Phys.* **46**, 1585 (1975).

17. F. Claro and G. D. Mahan, *J. Appl. Phys.* **66**, 4213 (1989).

18. K. Kinoshita, M. Ito, and Y. Suzuki, *Rev. Sci Instrum.* **58**, 932 (1987).